



RESEARCH ARTICLE OPEN ACCESS

Inhibition of the RNA Regulator HuR Mitigates Spinal Cord Injury by Potently Suppressing Post-Injury Neuroinflammation

Mohammed Amir Husain^{1,2,3} | Reed Smith^{1,2,3} | Robert E. Sorge^{3,4} | Abdulraheem Kaimari¹ | Ying Si^{1,2,3} | Ali Z. Hassan¹ | Abhishek Guha^{1,2,3} | Katherine A. Smith^{1,2} | Christopher P. Cardozo^{5,6} | Jennifer J. DeBerry^{3,7}  | Shaida A. Andrabi^{1,8} | L. Burt Nabors¹ | Natalia Filippova¹ | Caroline K. Webb⁴ | Peter H. King^{1,2,3,9} 

¹Department of Neurology, University of Alabama at Birmingham, Birmingham, Alabama, USA | ²Killion Center for Neurodegeneration and Experimental Therapeutics, University of Alabama at Birmingham, Birmingham, Alabama, USA | ³Birmingham Veterans Affairs Health Care System, Birmingham, Alabama, USA | ⁴Department of Psychology, University of Alabama at Birmingham, Birmingham, Alabama, USA | ⁵Spinal Cord Damage Research Center, James J. Peters VA Medical Center, Bronx, New York, USA | ⁶Department of Medicine, Icahn School of Medicine at Mount Sinai, New York, New York, USA | ⁷Anesthesiology and Perioperative Medicine, University of Alabama at Birmingham, Birmingham, Alabama, USA | ⁸Pharmacology and Toxicology, University of Alabama at Birmingham, Birmingham, Alabama, USA | ⁹Department of Cell Developmental, and Integrative Biology, University of Alabama at Birmingham, Birmingham, Alabama, USA

Correspondence: Peter H. King (phking@uabmc.edu)

Received: 23 January 2025 | **Revised:** 9 April 2025 | **Accepted:** 18 April 2025

Funding: This work was supported by U.S. Department of Veterans Affairs (VA) (BX005899 and BX006244).

Keywords: HuR translocation | neuroinflammation | RNA regulation | spinal cord injury | SRI-42127

ABSTRACT

Neuroinflammation is a major driver of secondary tissue damage after spinal cord injury (SCI). Within minutes after SCI, activated microglia and astrocytes produce proinflammatory mediators such as TNF- α , IL-6, iNOS, and COX-2 which induce tissue injury through cytotoxicity, vascular hyperpermeability, and secondary ischemia. The inflammatory cascade is amplified by chemokines like CCL2 and CXCL1 which recruit immune cells to the injured site. HuR is an RNA regulator that promotes glial expression of many proinflammatory factors by binding to adenylate- and uridylylate-rich elements in the 3' untranslated regions of their mRNAs. SRI-42127 is a small molecule which blocks HuR function by preventing its nucleocytoplasmic translocation. This study aimed to evaluate the potential of SRI-42127 to suppress neuroinflammation after SCI and improve functional outcome. Adult female mice underwent a T10 contusion injury and received SRI-42127 1 h post injury for up to 5 days. Locomotor function was assessed by open field testing, balance beam, and rotarod. Immunohistochemistry was used to assess lesion size, neuronal loss, myelin sparing, microglial/astroglial activation, and HuR localization. Inflammatory mediator expression was assessed by qPCR, immunohistochemistry, ELISA, or western blot. We found that SRI-42127 treatment significantly attenuated loss of locomotor function and post-SCI pain. There was a reduction in lesion size and neuronal loss with an increase in myelin sparing. Microglia and astrocytes showed reduced activation and reduced nucleocytoplasmic translocation of HuR. There was a striking suppression of proinflammatory mediators at the epicenter along with peripheral suppression of inflammatory responses in serum, liver, and spleen. In conclusion, HuR inhibition with SRI-42127 may be a viable therapeutic approach for suppressing neuroinflammatory responses after SCI and improving functional outcome.

This is an open access article under the terms of the [Creative Commons Attribution-NonCommercial-NoDerivs](https://creativecommons.org/licenses/by-nc-nd/4.0/) License, which permits use and distribution in any medium, provided the original work is properly cited, the use is non-commercial and no modifications or adaptations are made.

© 2025 The Author(s). *The FASEB Journal* published by Wiley Periodicals LLC on behalf of Federation of American Societies for Experimental Biology.

1 | Introduction

Traumatic spinal cord injury (SCI) is a debilitating neurological injury affecting more than 250,000 individuals per year globally. The injury often results in permanent disability and shortened lifespan. Additionally, there are life-changing socioeconomic consequences for both the individual and their caregivers, particularly younger people [1, 2]. Treatment in the acute phase of injury is mainly supportive, with limited options for neuroprotection to improve recovery and reduce long-term disability.

The physical trauma of SCI triggers a robust inflammatory response initiated within minutes by resident microglia and astrocytes in the vicinity of tissue injury. This activation leads to the production of proinflammatory mediators including IL-1 β , IL-6, TNF- α , MMPs, COX-2, and nitric oxide (NO) via iNOS which exert direct toxic effects on neurons, oligodendroglia, and endothelial cells and peak within the initial 24 h post injury [3, 4]. These mediators increase vascular permeability by disrupting the blood-spinal cord barrier (BSCB), leading to edema, secondary ischemia, and hemorrhage [5, 6]. Disruption of the BSCB, in combination with glial secretion of chemokines such as CCL2 and CXCL1, further intensifies the inflammatory cascade by facilitating the recruitment and infiltration of peripheral neutrophils and monocytes [3].

An integral regulatory component to this inflammatory cascade, beginning with activated microglia and astrocytes, is at the posttranscriptional level, where AU-rich elements (ARE) in the 3' untranslated region (UTR) of proinflammatory mRNAs govern their expression through modulation of RNA stability and translational efficiency [4]. HuR, a major cellular RNA-binding protein (RBP) in glial cells, binds to these AREs and positively regulates mRNA stability and translational efficiency leading to increased expression [4, 7–10]. Primarily located in the nucleus, HuR translocates to the cytoplasm upon activation where it transports and stabilizes bound mRNAs and facilitates their localization to polysomes for translation. In microglia and/or astrocytes, HuR translocation is triggered in different inflammatory conditions, including SCI [9, 11], amyotrophic lateral sclerosis [8], lipopolysaccharide (LPS) stimulation [10, 12], hypoxia [10], and glioblastoma [7]. Knockdown or deletion of HuR in microglia and astrocytes significantly diminishes the expression of many key inflammatory mediators, including proinflammatory cytokines, chemokines, and iNOS which are associated with secondary tissue injury in SCI [7–9]. Our group has recently developed a small molecule, SRI-42127, that blocks HuR dimerization, a process critical for nucleocytoplasmic shuttling and RNA binding [13–15]. SRI-42127 inhibits the translocation of HuR in microglial cells and astrocytes after activation with LPS and suppresses the production of proinflammatory mediators [10]. In our prior work, SRI-42127 potently attenuated the development of neuropathic pain in a peripheral nerve injury model, a process that is driven by neuroinflammatory responses in the spinal cord [16, 17]. With this background, we hypothesized here that inhibition of HuR with SRI-42127 would suppress neuroinflammatory responses after acute SCI, reduce secondary tissue injury, and mitigate loss of motor function.

2 | Methods

2.1 | Animals and the Contusion Model of Spinal Cord Injury

All animal procedures were approved by the UAB Institutional Animal Care and Use Committee and were carried out in accordance with relevant guidelines and regulations of the National Research Council Guide for the Care and Use of Laboratory Animals. Female C57/Bl6 mice (IMSR_JAX:000664) between 10 and 14 weeks of age were anesthetized under isoflurane, and a laminectomy was performed to remove the dorsal aspect of the T10 vertebrae. The animal was transferred to a spinal stereotaxic frame and clamps were attached to the T9 and T11 vertebral spines to secure the vertebral column. Using a 0.8-mm diameter tip, a single impact contusion of 50 kdyn was delivered using the Infinite Horizon spinal cord injury device (Precision Systems & Instrumentation, Lexington, KY). Sham control mice received a laminectomy only. Post-operatively, animals received manual bladder evacuation twice daily to prevent urinary tract infections. One dose of subcutaneous buprenorphine was administered prior to injury and every 12 h for 3 days post injury. For molecular studies, SRI-42127 (10 mg/kg) and vehicle were prepared as previously described [16] and administered intraperitoneally every 2 h beginning 1 h after injury for 4 doses. The cohort for behavioral studies received 4 doses daily, starting 1 h after injury, for 5 days. Sample size was based on estimations by power analysis to achieve a power of 0.8 at a significance of 0.05.

2.2 | RNA Isolation and qPCR

The thoracic spinal column was harvested, and 2 mm sections were cut from the epicenter of injury and adjacent rostral and the caudal spinal column. Spinal cord was removed from these sections, and RNA was isolated using the TRIzol reagent as per the manufacturer's protocol (Thermo Fisher Scientific). RNA was precipitated using isopropanol (Sigma) and glycogen (Thermo Fisher Scientific), and concentrations were measured by Nanodrop (Thermo Scientific, Waltham, MA; RRID:SCR_016517). Complementary DNA was reverse transcribed from 2 μ g of total RNA using a reverse transcription kit (Thermo Fisher Scientific). Quantitative Real Time PCR (qRT-PCR) was conducted using the ViiA7-Real-Time PCR system and primers and probes from Applied Biosystems as previously described [10].

2.3 | Western Blot and ELISA

For western blotting, whole cell lysates were prepared using T-PER (ThermoFisher), and quantification was done with a BCA protein assay kit (ThermoFisher). Fifty μ g of protein per sample were electrophoresed in a 4%–20% mini-PROTEAN gel (Biorad) and transferred to a nitrocellulose membrane. Blots were immunostained with a COX-2 antibody (Santa Cruz Biotechnology, USA; RRID:AB_2722522) was used at a dilution of 1:1000. Each sample was analyzed in triplicate and quantified using Image lab software (Bio-Rad Laboratories, USA Inc.). For ELISA of peripheral serum samples, cytokines (IL-1 β , IL-6, IL-10, TNF- α , CCL2, and CXCL1) were

measured using U-plex biomarker Group 1 (mouse) Assays (K15069M, MSD). Analyses were done using a QuickPlex SQ 120 instrument (MSD) and DISCOVERY WORKBENCH 4.0 software (MSD).

2.4 | Immunohistochemistry

Mice were euthanized 8 h or 3 weeks and perfused with an ice-cold phosphate buffer saline (PBS) solution for 2 min followed by a 4% paraformaldehyde (PFA) solution for 5 min [9]. The entire spinal column was then extracted and post-fixed in PFA for 24 h before being decalcified with 8% hydrochloric acid and 10% ethanol in PBS. The spinal column was incubated in a PBS solution with 10% sucrose for cryoprotection and then transferred to a 30% sucrose in PBS solution for 48 h. Two mm samples of the spinal column from the epicenter and adjacent rostral (+ 2 mm) and caudal tissues (−2 mm) were preserved and cryo-molded in OCT. A cryostat was used to cut samples into 30 μm serial sections cut transversely.

Sections were washed with PBS and blocked in 10% goat serum for 1 h. Samples were incubated overnight with primary antibodies (GFAP, 1:500, Z0334, Dako, Carpinteria, CA; RRID:AB10013382), (Iba1, 1:500, FUJIFILM Wako Chemicals U.S.A. Corporation; RRID:AB839504), (NeuN, 1:400, ABN78, Sigma-Aldrich, USA Ltd.; RRID:AB10807945), (HuR, 1:500, sc-5261, Santa Cruz Biotechnology, USA Inc; RRID:AB_627770). The following day, slide sections were washed and incubated with Alexa fluorophore-conjugated secondary antibodies (Goat anti mouse, A28175, Thermo Fisher Scientific, RRID:AB_2536161; Goat anti rabbit Cy3, 111-165-144, Jackson Immuno Research, RRID:AB_2338006) for 2 h and mounted with antifade DAPI + mountant (ThermoFisher Scientific P36966). For myelin staining, sections were incubated with FluoroMyelin Green for 20 min (1:300, Invitrogen).

Quantitative assessment of HuR localization was done using our previously published method [10]. Fiji software (RRID:SCR_002285) was utilized for image analysis, and a minimal threshold was established in order to quantify the mean fluorescence intensity (FI). FI was quantified and normalized with the DAPI FI for the same region and expressed as arbitrary units (AU). Total lesion area was determined based on the ratio of GFAP-stained area (which is concentrated on the border of the injured region) to total spinal cord area. The total area of GFAP and myelin staining was measured using the freehand selection tool and threshold functions in Fiji. Three biological replicates were used for the Fiji analysis.

2.5 | Analysis of Microglial Morphology

During the early stages of activation, microglia can become hyper-ramified with increased branch complexity and soma enlargement [18, 19]. Fiji software (<https://imagej.net/>) was used to convert all photomicrographs to binary and skeletonized images using the AnalyzeSkeleton plugin (<https://imagej.net/plugins/analyze-skeleton/>). To analyze the number of branches, the total branch length, and the endpoints per microglia, brightness and contrast are changed by updating the Fiji lookup table, so

pixel values are unchanged. This is followed by a despeckle step to remove salt-and-pepper noise. Photomicrographs are then converted to binary using the threshold tool, followed by skeletonizing the image using the toolbar Skeletonize and AnalyzeSkeleton (2D/3D) to collect data on the branch length. Branch length per cell was calculated by dividing the summed branch length by the number of microglia somas in the corresponding photomicrographs. Data were obtained from 5007 microglial cells from vehicle control ($n = 3$) and 4538 microglial cells from SRI-42127 ($n = 3$). The soma area was calculated using the Fiji multipoint area selection tool.

2.6 | Open Field Test

Motor function of the hind limbs was scored at 1, 2, and 3 weeks after SCI using the open-field basso mouse scale (BMS) in 10 min observation periods. BMS is a reliable measure and has been widely used to evaluate motor functions after SCI in mice [20]. Briefly, each mouse was separately placed in an open field (60 cm × 120 cm) and patterns of limb movement such as ankle movement, plantar placing and stepping of paw, paw positions, and trunk instability were recorded over a 10 min time interval by a ceiling camera and analyzed by a computerized tracking system, EthoVision XT software (Noldus, USA RRID:SCR_000441). Prior to the testing day, baseline measurements were obtained. Videos were carefully inspected by two reviewers (MAH and HAZ) blinded to the experimental conditions. Hindlimb joint movement, coordination, and weight support were evaluated using a rating scale from 0 points (no movement of any kind) to 9 points (normal locomotion). EthoVision software was used to analyze recorded videos to automatically calculate total distance traveled, mobility, and velocity by each mouse within the arena.

2.7 | Beam Walking

The apparatus consists of a round horizontal beam of 100 cm long and 1.2 cm in diameter and was elevated 50 cm above the ground. A hollow black escape box was attached to one end of the beam. One fluorescent lamp (60 W) was used to illuminate the beam from the start side. One week prior to SCI, mice were thoroughly trained to traverse the beam from the start point to the end point (black box). Baseline measurements were taken 1 day before the SCI. On the trial days after SCI, mice were placed at the start point and were allowed to walk for 2 min for 3 trials. The test was recorded by a video camera. A score was given to the mice as described elsewhere [21]. Briefly, the rating system employs values such as mouse retention, forward motion, and goal achieving on a beam. Mice received a high score for effectively using their hindlimbs to move around the beam. When there was absence of hindlimb movements, a score of 0 was given. Scoring was done by an observer blinded to the identity of the mouse using recorded video at weeks 1, 2, and 3 after SCI. A mean value was calculated from the three trials for each mouse.

2.8 | Rotarod

Motor coordination was assessed in weeks 1, 2, and 3 post SCI on an accelerating rotarod (San Diego instruments CA,

USA). Mice were trained 1 week before SCI by placing them on the revolving rotor (4 rpm) and allowing them to acclimate for 2 mins. Baseline measures were acquired 1 day prior to the contusion injury. On the day of testing the rod accelerated from 4 to 60 rpm over 2 mins, and the latency to fall off was measured in 2 trials on each testing day, allowing them 5 min of rest in between each trial. The average time for the 2 trials was used for statistical analysis to calculate a single score for each mouse.

2.9 | Non-Evoked Pain Testing

Mice were placed into tabletop plexiglas cubicles (12×8×5.5 cm) with perforated metal floors and clear walls. High-resolution (1920×1080) cameras (Sony Handycam model HDR-CX100) were set up in front of and behind the cubicles as described elsewhere [22]. After 15 min of habituation, cameras were turned on to record for 15 mins. Recordings were taken prior to surgery (baseline, BL) and at days 2 and 9 post SCI. Still images with clear visuals of the face were taken once in each 2-min period for each recording (8 images total) by an experimenter blinded to the group assignment. Images were added to a PowerPoint file, randomized, and scored by two observers blinded to the experimental conditions. Scores for action units were averaged within each recording session. Action unit scores were averaged to calculate a mouse grimace score (MGS).

2.10 | Statistics

All statistical analyses were performed by Graphpad (GraphPad Software Inc.). The mean values are shown on graphs along with error bars with error bars reflecting standard deviation or standard error as indicated. An unpaired Welch's *t* test was used for HuR localization, qPCR, western blot, FI, and microglia counting. Two-way ANOVA with Tukey post hoc test was used for CCR2. Data from all behavioral testing were analyzed using an unpaired Welch's *t* test. A *p*-value less than 0.05 was considered statistically significant.

3 | Results

3.1 | SRI-42127 Treatment Improves Functional Recovery After SCI

Wild-type female mice were subjected to a mid-thoracic contusion injury and then treated with SRI-42127 every 6 h for 5 days, starting 1 h after injury. To assess and quantitate motor activity over a longer period of time, we used a computerized tracking system in an open field (Figure 1). We first assessed locomotor function using the Basso mouse scale (BMS) at weeks 1, 2, and 3 post SCI (Figure 1A). There was a highly significant increase in BMS scores for drug-treated mice versus vehicle beginning at week 1 (4.2 ± 1.2 versus 0.2 ± 0.1 ; $p < 0.0001$). The separation of BMS scores persisted and remained significant in weeks 2 and 3, with both groups showing some recovery by week 3. Heat maps of activity within the field were generated (example shown in Figure 1B) from which distance moved,

mobility, and velocity were calculated (Figure 1C–E). At week 1, there was more than a two-fold increase in distance moved (3900 ± 200 versus 1800 ± 100 cm; $p < 0.0001$), mobility (6.5 ± 0.7 versus $4.0\% \pm 0.5\%$; $p = 0.0029$), and velocity (6.8 ± 1.0 versus 3.0 ± 0.5 cm/s; $p < 0.0001$). The differences between drug- and vehicle-treated groups remained significant throughout the recovery period for each parameter, with both groups showing improvement by week 3. We next assessed the animals with a novel beam walking test which quantifies locomotor recovery using a scale of 0 to 7 (Figure 1F) [21]. This test provides a more comprehensive assessment of beam walking by measuring other functional components besides latency to reach the other side. In both test groups, pre-injury baseline (BL) scores were 7. At week 1, there was a significant increase in score in the SRI-treated group compared to vehicle (3.3 ± 1.2 versus 0.6 ± 0.2 ; $p < 0.0001$). This difference persisted throughout the three-week observation period, with both groups showing modest improvement by week 3 (5.0 ± 1.2 versus 2.0 ± 0.5 ; $p < 0.0001$). Next, we assessed rotarod performance (Figure 1G) and found that SRI-treated mice had a ~5-fold increase in mean latency to fall at week 1 compared to vehicle control (6.8 ± 3.1 versus 1.3 ± 1 ; $p = 0.0012$). This difference remained significant throughout the recovery period, with both groups showing increases in latency by week 3. To exclude the possibility of a drug effect on motor function, independent of SCI, we performed open field testing, BMS, and beam walking on sham-injured mice given SRI-42127 and observed no difference compared to the vehicle group over the 3-week testing period (Figure S1). Since pain is a common and debilitating sequela of SCI, we assessed non-evoked pain using the mouse grimace scale (MGS) (Figure 1H). At baseline, prior to SCI, the groups had similar MGS scores (0.31 ± 0.02 versus 0.29 ± 0.04). Following SCI, mice treated with SRI-42127 had significantly lower MGS scores when compared to vehicle-treated mice (day 2: 1.56 ± 0.11 versus 1.02 ± 0.09 , $p < 0.01$; day 9: 0.83 ± 0.08 versus 0.46 ± 0.05 , $p < 0.01$). Taken together, SRI-42127 treatment after SCI significantly attenuated motor function loss and pain.

3.2 | SRI-42127 Mitigates Histopathological Changes After SCI

At 3 weeks post SCI, spinal cords were harvested and tissue sections at the epicenter and adjacent rostral and caudal levels were examined for histopathological changes. To identify the glial scar border, we immunostained sections with GFAP (Figure 2A). Using these borders, a lesion size was calculated and found to be reduced by 60% in drug-treated mice versus vehicle ($p = 0.003$) (Figure 2B). Inspection of rostral and caudal levels revealed no evidence of glial scar (Figure S2A). To assess for neuronal loss, sections were immunostained with NeuN (Figure 2C). In drug-treated mice, there was a 7-fold increase in NeuN positive cells in the epicenter (Figure 2D; $p = 0.003$). Overall NeuN fluorescence intensity (FI) was significantly higher in drug-treated mice (Figure 2E). In rostral and caudal levels, there were no differences in NeuN FI (Figure S2B). We next stained sections from the epicenter with fluoromyelin to assess white matter sparing at 3 weeks (Figure 2F,G). There was a 4.5-fold increase in Fluoromyelin FI in drug-treated mice versus vehicle ($p = 0.003$) consistent with myelin sparing. In rostral and caudal levels, there was also a 40%–50% increase in FI ($p < 0.01$) in drug-treated mice (Figure S2C).

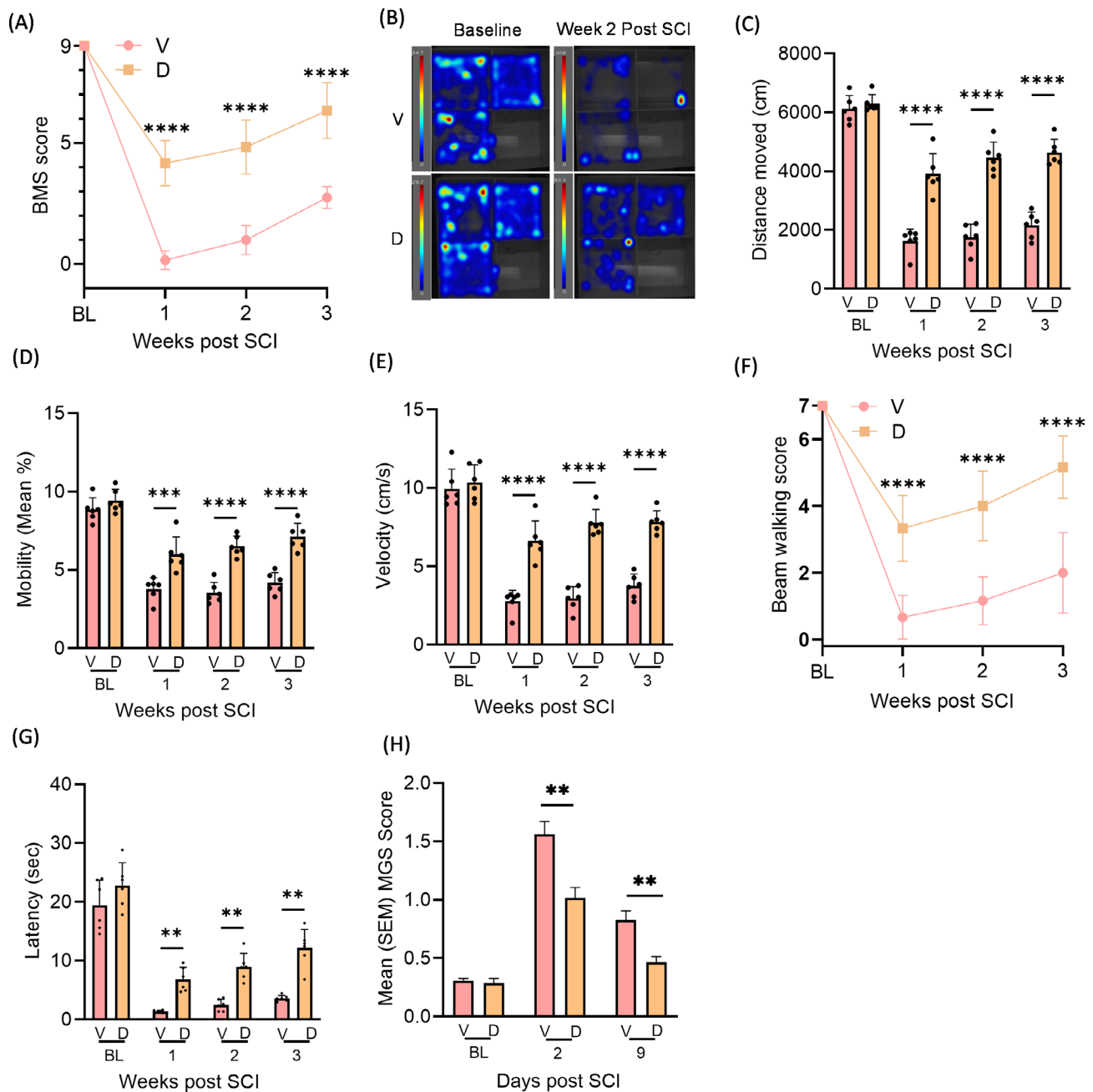


FIGURE 1 | SRI-42127 attenuates motor function loss and pain after SCI. Following SCI, SRI-42127 (10mg/kg) or vehicle was administered IP at 6 h intervals for 5 days starting 1 h after injury. (A) BMS scores for vehicle control and drug-treated mice were measured at 1, 2, and 3 weeks after SCI. (B) Motor function post SCI was assessed by open field testing. A representative heat map of activity at 2 weeks post SCI is shown. Different parameters of motor activity were measured including (C) distance moved, (D) mobility, and (E) velocity. (F) Beam walking scores of vehicle and drug-treated mice were obtained at 1, 2, and 3 weeks post SCI. (G) Rotarod testing was performed at 1-, 2-, and 3-weeks post SCI and latency to fall was measured. (H) Non-evoked pain was assessed by mouse grimace scores (MGS) which were measured at day 2 and 9 post SCI. Baseline testing of both test groups, prior to SCI, had similar MGS scores. Evaluations for open field BMS, beam walking, and non-evoked pain were made by two observers blinded to the status of the animal. Error bars represent means \pm SD of 6 mice/group. ** $p < 0.01$, *** $p < 0.001$, **** $p < 0.0001$.

3.3 | SRI-42127 Blocks Nucleocytoplasmic Translocation of HuR in Microglia and Attenuates Microglial Activation

A hallmark of HuR activation is its translocation from the nucleus to the cytoplasm where it stabilizes and promotes the translational efficiency of proinflammatory mediators in microglial cells [4, 10]. Here, we assessed HuR localization by

immunohistochemistry in Iba1+ cells at 8 h post-SCI. At the epicenter, there was prominent HuR translocation in vehicle-treated mice, as indicated by a merged signal with cytoplasmic Iba1 (Figure 3A, Figure S3). This shift was not seen in uninjured rostral or caudal levels (Figure S4). In drug-treated mice, this merged signal was not observed (Figure 3B). A nuclear/cytoplasmic ratio of HuR FI was calculated and found to be more than 2-fold higher in drug-treated mice ($p = 0.002$)

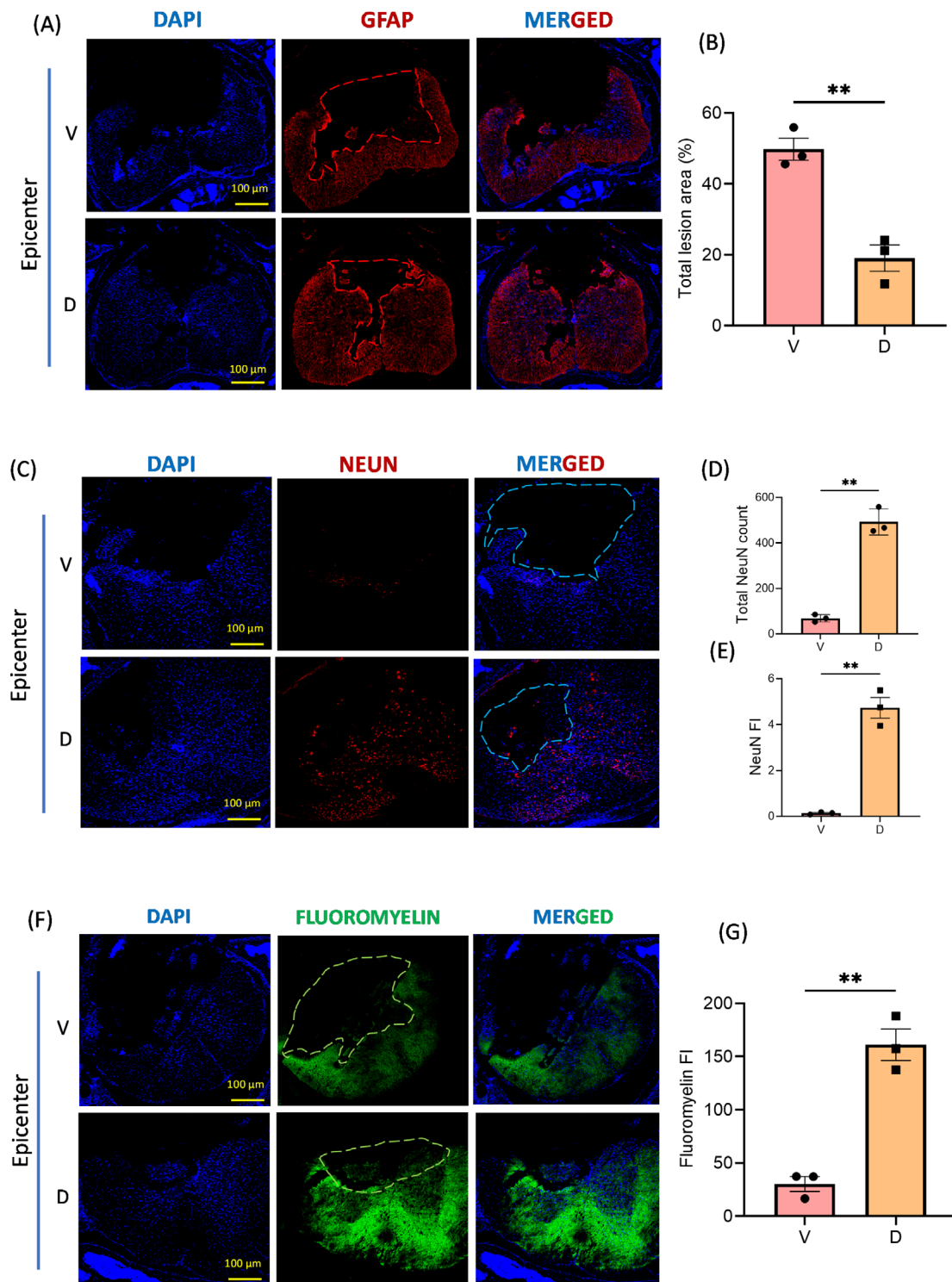


FIGURE 2 | SRI-42127 treatment reduces lesion size and loss of neurons after SCI while increasing myelin sparing. (A) Representative GFAP-immunostained sections from the epicenter (3 weeks post SCI) showing reduced lesion size in a drug-treated mouse compared to vehicle control. (B) Total lesion area was quantified in 3 vehicle and 3 drug-treated mice. (C) Representative NeuN-immunostained sections from the epicenter showing an increase in NeuN+ cells in the drug-treated mouse. (D) NeuN+ cells were quantified at the epicenter in 3 vehicle and 3 drug-treated mice at 3 weeks post-SCI. (E) NeuN fluorescence intensity (FI) was quantified at the epicenter. (F) Representative fluoromyelin-stained sections from the epicenter showing increased myelin staining in the drug-treated mouse compared to vehicle control. (G) Fluoromyelin staining at the epicenter was quantified in 3 vehicle and 3 drug-treated mice. Dashed lines delineate the boundary of the injured spinal cord. Bars represent the mean \pm SD of 3 mice/group. ** $p < 0.01$. Scale bars 100 μ m.

consistent with nuclear retention of HuR (Figure 3C). To assess microglial activation, we measured Iba1 FI for individual cells in the epicenter and found an overall reduction in drug-treated

mice consistent with reduced activation (Figure 3D). This was underscored by a reduction in total Iba1 FI (Figure 3E) as the overall Iba1+ cell count was unchanged (Figure 3F).

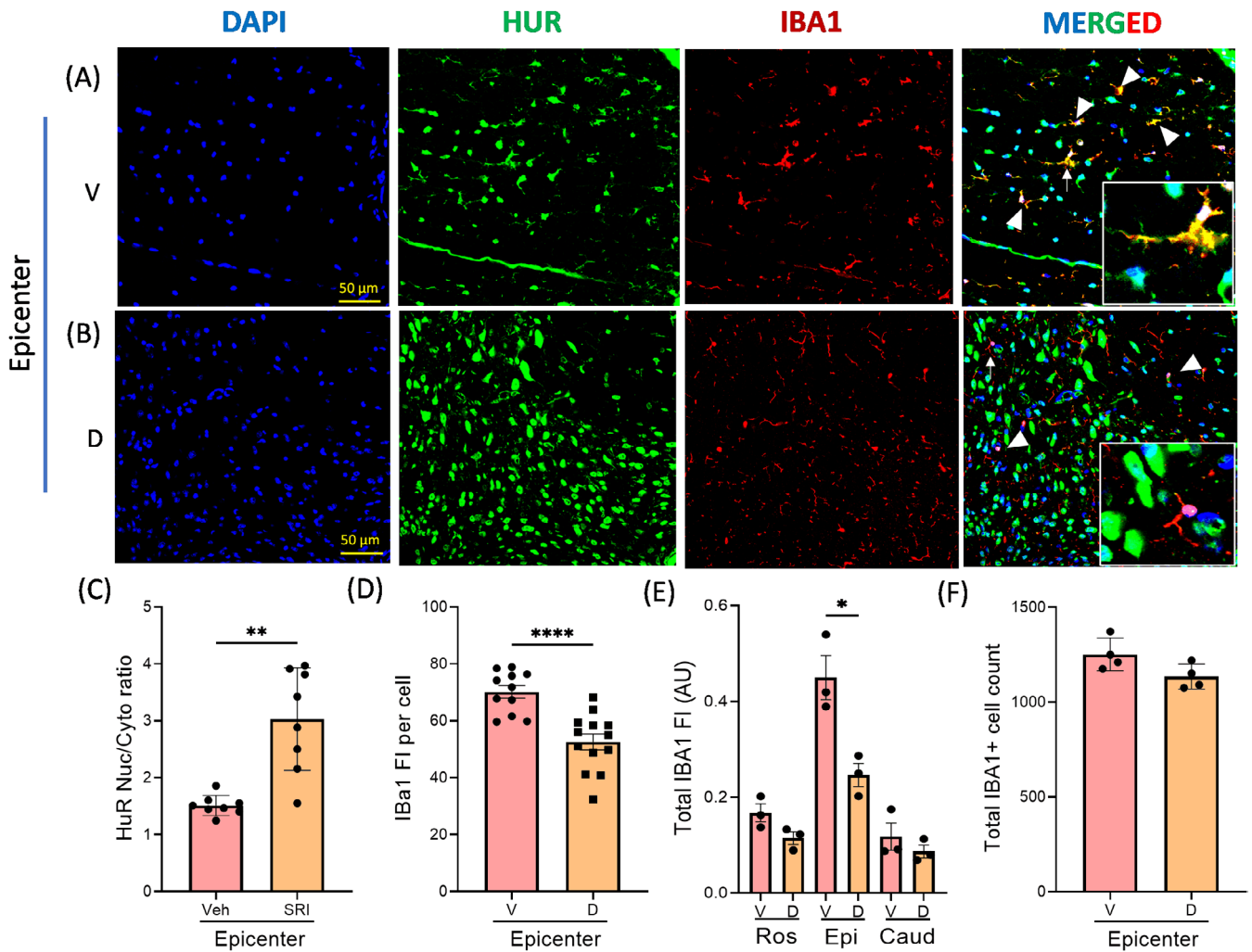


FIGURE 3 | SRI-42127 inhibits nucleocytoplasmic translocation of HuR in microglia and attenuates microglial activation. Eight hours after SCI, sections from the epicenter were immunostained with antibodies as shown. (A) Cytoplasmic translocation of HuR is observed in microglia at the epicenter in a vehicle-treated mouse as indicated by a merged yellow signal of HuR and Iba1 (arrowheads). A higher power view of a microglial cell (arrow) is shown in the insert. (B) SRI-42127 treatment blocked HuR translocation from the nucleus as indicated by a merged signal of HuR and DAPI (arrowheads) and the absence of a merged yellow signal. A higher power view of a microglial cell is shown in the inset. (C) Microglial HuR localization was quantified from 4 biological replicates as described in the Methods and expressed as a nuclear/cytoplasmic ratio. (D) Quantification of Iba1 fluorescence intensity (FI) from 3 biological replicates. (E) Total Iba1 FI was quantified at the epicenter, rostral, and caudal levels. (F) Total Iba1+ cell counts at the epicenter were quantified in 3 biological replicates. * $p < 0.05$, ** $p < 0.01$, **** $p < 0.0001$. Scale bars 50 μm , 10 μm (insets).

Iba1 FI in rostral and caudal segments showed no differences between drug-treated and vehicle control mice (Figure 3E). Interestingly, we did not see translocation of HuR in astrocytes in vehicle-treated mice at this early timepoint but did at 24 h (Figure S5A versus 5B). GFAP FI, however, was increased by 5-fold at the epicenter compared to caudal segments in vehicle-treated mice which was decreased by ~55% with SRI-42127 treatment (Figure S5C). Rostral levels also showed reduced GFAP FI in drug-treated mice. In summary, SRI-42127 suppressed SCI-induced HuR nucleocytoplasmic translocation in microglial cells and astrocytes as well as their activation.

3.4 | SRI-42127 Attenuates Activation-Associated Microglial Morphological Changes

As another measure of activation, we assessed morphological changes of microglia at the epicenter 8 h after SCI. Using Fiji

software, a skeleton analysis of microglia was done as previously described [23] (Figure 4A). We observed a decrease in branch length ($p = 0.009$), number of branches ($p < 0.0001$), and number of end points per microglia ($p < 0.0001$) in drug-treated mice, consistent with reduced early-stage activation [24]. In addition to hyper-ramification, we measured soma size as an indicator of reactive microglia and found a > 2-fold reduction in drug-treated mice (Figure 4B; $p < 0.0001$). Taken together, SRI-42127 attenuates some of the morphological features of microglial activation after SCI.

3.5 | SRI-42127 Suppresses Induction of Proinflammatory Mediators at the Epicenter of SCI

At 8 h post-SCI, spinal cords were harvested and divided into 3 segments: injury epicenter, rostral, and caudal. RNA expression

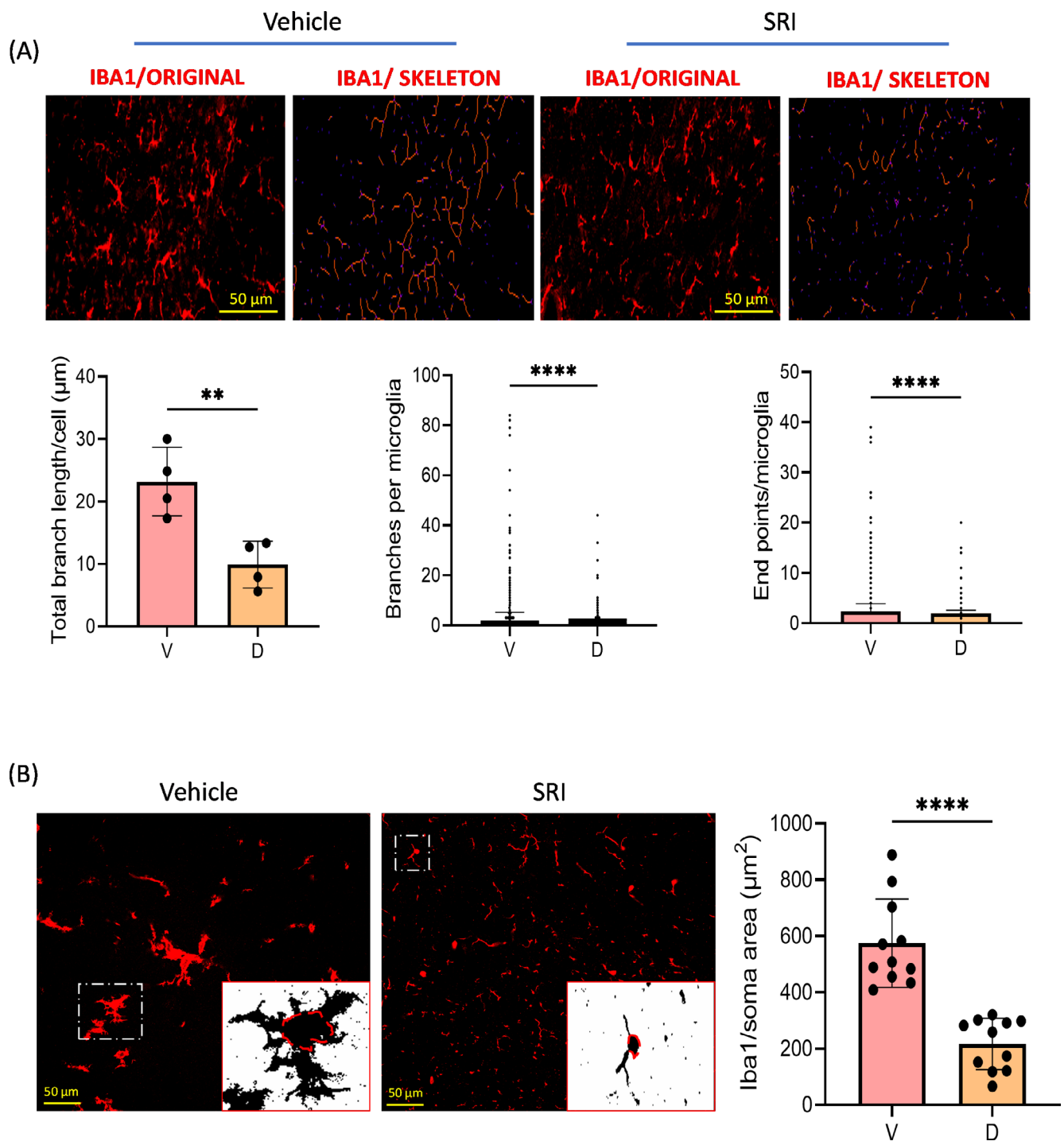


FIGURE 4 | SRI-42127 attenuates activation-associated changes in microglial morphology after SCI. (A) Eight hours after SCI, tissue sections from the epicenter were immunostained with Iba1 antibodies and digitally converted to Skeletonized images using Fiji software. Representative images are shown. Morphological features were quantified, including total microglia branch length, number of branches per microglial cell, and number of branch endpoints per microglial cell. Data were generated from 5007 microglial cells from vehicle control ($n = 3$ biological replicates) and 4538 microglial cells from SRI-42127 ($n = 3$ biological replicates). (B) The soma of Iba1+ microglial cells was identified as shown in the representative images to the left. Binary images were generated by adjusting the Fiji threshold level (shown in inserts). Total area was quantified in 11 cells from 3 biological replicates, as shown in the graph. Error bars represent SD. ** $p < 0.01$, **** $p < 0.0001$.

of proinflammatory mediators was assessed by qPCR. At the epicenter, there was a large induction of *IL-6*, *IL-1β*, *TNF-α*, *CCL2*, *MMP12*, *CXCL1*, *CXCL2*, and *iNOS* in the vehicle control compared to rostral and caudal segments (Figure 5A). *COX2* and *TGF-β1* mRNAs were not induced. The induction was most pronounced with *IL-6* (34-fold) and *CXCL2* (39-fold) while the others

ranged from 5- to 15-fold. SRI-42127 treatment suppressed the expression of all proinflammatory mediators, most potently for *IL-6* (~13-fold) and *IL-1β* (~9-fold). Other inflammatory mediators were suppressed by 3- to 7-fold. Interestingly, there was drug-induced suppression of some mRNAs at non-injured spinal cord segments, including *IL-1β*, *CCL2*, *MMP-12*, and *CXCL1*.

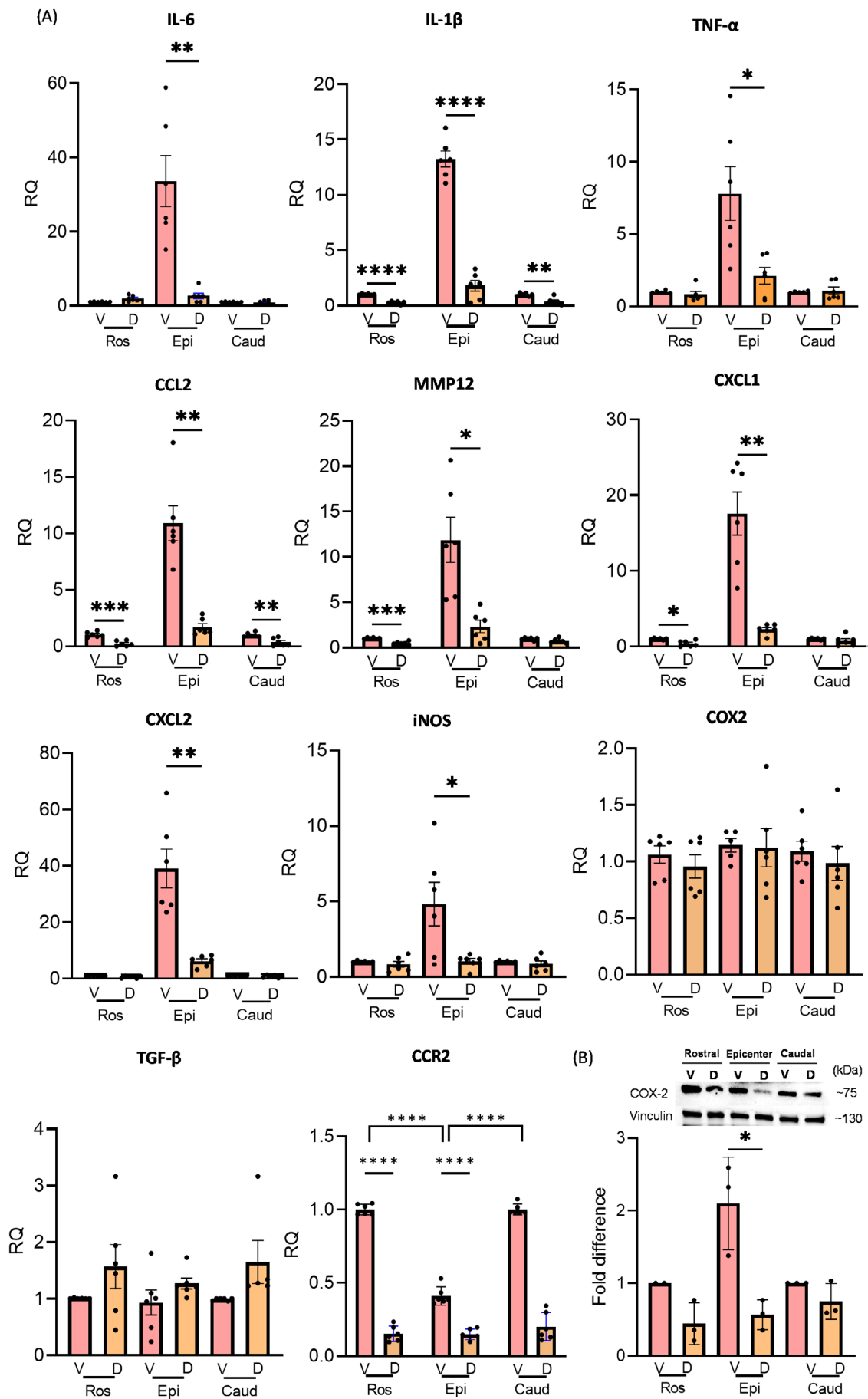


FIGURE 5 | Legend on next page.

FIGURE 5 | SRI-42127 attenuates pro-inflammatory cytokine and chemokine mRNA induction. (A) Spinal cords were harvested at 8 h post-SCI and divided into 3 segments: Injury epicenter, rostral, and caudal. RNA expression of proinflammatory cytokines and chemokines was assessed by qPCR in vehicle controls and SRI-42127 treated mice. All values were expressed relative to the vehicle control, which was set at 1.0. GAPDH was used as the housekeeping control. * $p < 0.05$, ** $p < 0.01$, *** $p < 0.001$, **** $p < 0.0001$. Error bars represent means \pm SEM of 6 mice/group. (B) COX-2 western blot of protein lysate from epicenter, rostral, and caudal spinal cord levels obtained 8 h after SCI. A representative blot is shown above. COX-2 levels were quantified by densitometry from three biological replicates using vinculin as a loading control. All values were expressed relative to the vehicle controls at rostral and caudal segments, which were set at 1.0. Error bars represent the mean \pm SD. * $p < 0.05$.

Based on our prior work showing that HuR positively regulates *CCR2* in microglia [8], we assessed this mRNA after injury and found a nearly 3-fold attenuation at the epicenter. SRI-42127 suppressed *CCR2* mRNA at the uninjured levels as well. The fold-change was even larger as there was significantly higher expression of *CCR2* in non-injured levels for the vehicle control. Since COX-2 is heavily regulated by HuR at the translational efficiency level [25, 26], we assessed protein levels by western blot (Figure 5B). We found a 2-fold increase in COX-2 protein levels in vehicle-treated mice compared to uninjured levels, and this was attenuated by ~4-fold in drug-treated animals. To determine the impact of SRI-42127 on inflammatory cytokine induction at a later time point, we assessed spinal cords after 5 days of SRI-42127 or vehicle treatment (Figure S6). There was a sustained suppression of proinflammatory mediators, most potently for *MMP-12* (~90-fold) and *CXCL2* (~30-fold). Others were suppressed by 3- to 9-fold. *TGF- β 1*, on the other hand, was greater in vehicle-treated mice by ~3-fold. No difference was seen with *IL-1 β* while *CXCL1*, *iNOS*, and *COX-2* trended toward suppression but did not reach significance. Taken together, treatment with SRI-42127 in the acute phase of SCI broadly suppressed the induction of proinflammatory mediators at the level of injury.

3.6 | SRI-42127 Attenuates Peripheral Inflammatory Responses After SCI

We next examined the effects of SRI-42127 on peripheral inflammatory responses at 8 h post SCI (Figure 6). We first looked at circulating levels of key inflammatory mediators and found a large increase in IL-6 (5.8 vs. 6719 pg/mL) and CXCL1 (32.7 vs. 3268) in vehicle-treated mice after SCI compared to sham-injured mice (Figure 6A). CCL2 also increased by 3-fold (226 vs. 77.2 pg/mL). With SRI-42127 treatment, there was a significant attenuation of these inflammatory mediators: IL-6 (~5-fold; $p < 0.0001$), CXCL1 (~3.5-fold; $p < 0.0001$), and CCL2 (~2.5-fold; $p = 0.003$). While there were some increases in IL-10, TNF- α , and IL-1 β in vehicle-treated mice after SCI compared to sham-injured mice, SRI-42127 did not affect these changes. To gain insight into potential sources for these cytokines, we looked at the liver and spleen, two organs that drive the influx of inflammatory macrophages after SCI (Figure 6B) [27, 28]. In liver tissue, we observed a significant induction of *CXCL1* (~16-fold) and *IL-6* (9-fold) mRNA, which was suppressed by ~16-fold and 11-fold, respectively, with SRI-42127 treatment. For splenic tissue, there was an increase in *CCL2* (~16-fold) and *IL-6* (~10-fold) mRNA expression, which was suppressed by ~16-fold and ~8-fold, respectively, with SRI-42127 treatment. For cytokines that were not elevated in serum, including IL-1 β , TNF- α , and IL-10, there was only minimal induction of TNF- α in the liver compared to sham injury (Figure S7).

4 | Discussion

A major challenge in therapeutically targeting the inflammatory cascade after SCI is the heterogeneity and complexity of signaling pathways driven by the broad range of proinflammatory mediators induced after injury [3, 29, 30]. These pathways are numerous, often overlapping, and orchestrated by many cell types at different stages of acute injury, including microglia, macrophages, neutrophils, and astrocytes [30, 31]. HuR is a major RNA regulator of many proinflammatory mediators and is expressed in these cell types, making it a rational target for maximizing suppression of multiple components in the inflammatory cascade [3, 4, 7, 30, 32, 33]. In this report, we have shown that inhibiting HuR with the small molecule SRI-42127 potently suppresses proinflammatory responses in the spinal cord and periphery in the acute phase of SCI, resulting in a significant attenuation of motor function loss and neuropathic pain. Histologic correlates for this therapeutic effect include sparing of neurons and white matter at the level of injury, reduced lesion size, and reduced microglial and astrocyte activation.

A deleterious effect of glial HuR in SCI was first reported by our group using a transgenic mouse model where selective overexpression in astrocytes accentuated spinal cord edema, neuronal loss, and neuroinflammatory responses after acute injury [9, 11]. In those reports, we described prominent nucleocytoplasmic translocation of both endogenous and transgenic HuR similar to what we observed in microglia and astrocytes in the current work. In glial cells, HuR is predominantly nuclear in localization, but upon activation by triggers such as LPS [10], hypoxia [10], glioblastoma [7, 32], and amyotrophic lateral sclerosis [8], it translocates to the cytoplasm to promote stabilization and translational efficiency of proinflammatory mediator mRNAs [4, 32]. HuR translocation was prominent in microglia/macrophages and astrocytes at the epicenter early in the injury but not rostrally or caudally, indicating a specificity of activation to the level of trauma. In astrocytes, HuR translocation occurred by 24 h post SCI, consistent with our previous reports [9, 11], but not at 8 h, suggesting that microglial HuR is activated earlier in SCI. In both cell types, however, SRI-42127 attenuated cytoplasmic HuR which is consistent with the mechanism of blocking HuR translocation [10, 13–15].

Inhibition of HuR with SRI-42127 led to a striking suppression of two cytokines, IL-6 and IL-1 β , at the epicenter, both of which are rapidly induced within 1–3 h after injury [29]. These cytokines are considered key initiators of the inflammatory cascade and directly produce toxic effects on neurons, oligodendrocytes, and endothelial cells, leading to apoptosis and necrosis [30]. They are mainly produced by microglia

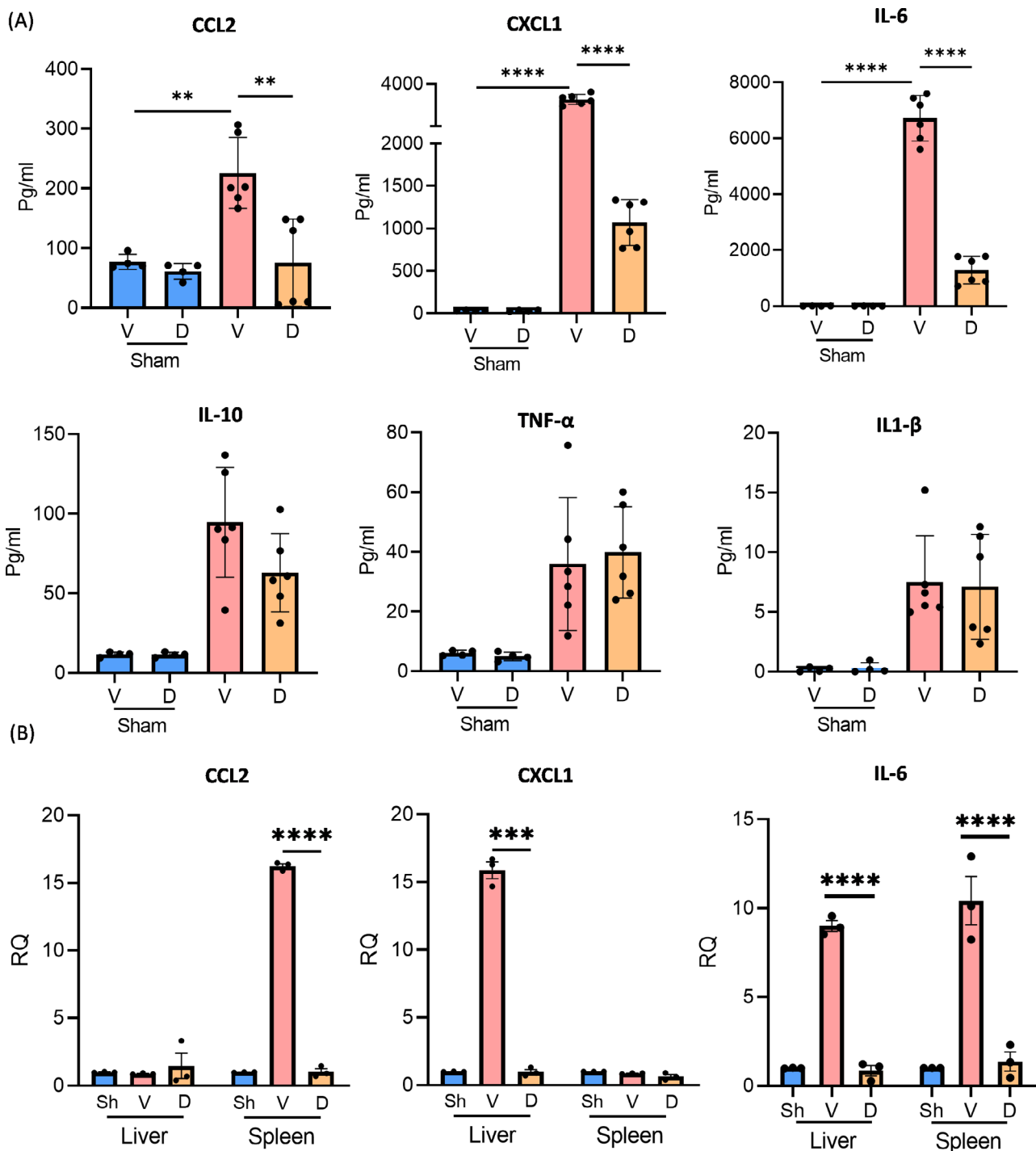


FIGURE 6 | SRI-42127 suppresses expression of pro-inflammatory mediators peripherally. (A) ELISA was used to quantify cytokines in plasma samples obtained at 8 h post SCI or sham (Sh) injury with vehicle (V) or SRI-42127 (D) treatment. (B) At the same time interval, RNA was harvested from liver and spleen and assessed by qPCR for CXCL1, CCL2, and IL-6 mRNA expression. Data represent the mean \pm SD of 6 mice/group for plasma and \pm SD of 3 mice/group for liver and spleen. ** $p < 0.01$, *** $p < 0.001$, **** $p < 0.0001$.

and astrocytes activated upon exposure to damage-associated molecular patterns (DAMPs) produced by the injury [4, 30]. This profound suppression is consistent with our prior studies showing that SRI-42127 had the greatest effect on IL-1 β and IL-6 induction in primary microglia and astrocytes after LPS stimulation and in spinal cord microglia after spared nerve injury (SNI) [10, 16]. In the SNI model, SRI-42127 treatment significantly reversed allodynic pain in the acute and chronic

phases of the injury [16]. IL-6 and its signaling pathway are causally linked to neuropathic pain in SCI [34–36]. Blocking the signaling pathway with a neutralizing antibody to the IL-6 receptor or inhibiting the downstream transducer, JAK2, abrogates the development of pain and improves functional recovery. Thus, the early and marked suppression of IL-6 in the epicenter of SRI-42127-treated mice may underlie the significant attenuation of spontaneous pain we observed after SCI.

SRI-42127 also suppressed proinflammatory mediators that enhance the inflammatory cascade and toxic microenvironment via different pathways, including iNOS (via nitric oxide), COX-2 (via PGE₂), and MMP-12 [3, 29, 30, 37, 38]. Interestingly, COX-2 protein but not mRNA was suppressed with SRI-42127 treatment. This may be related to a loss of translational efficiency rather than mRNA stability (and decrease in mRNA levels) as both processes represent two distinct posttranscriptional levels of regulation governed by HuR [4]. We have shown previously that these mediators are regulated by HuR in glial cells in different inflammatory environments and suppressed either by SRI-42127, MS-444 (another chemical HuR inhibitor [15]), or with HuR silencing/deletion [7–10, 16, 39]. In addition to direct toxic effects, these inflammatory mediators also trigger indirect toxicity by promoting vascular permeability, edema, ischemia, and hemorrhage [1, 30].

In the acute phase of injury, the inflammatory cascade is further amplified by glial and macrophage production of chemokines, particularly CXCL1, CXCL2, and CCL2, which promote the recruitment and activation of neutrophils, monocyte/macrophages, and other immune cells from the periphery [1, 30]. These chemokines were likewise suppressed by more than 6-fold with SRI-42127 treatment. In a compressive model of SCI, depletion of CCL2+ microglia significantly attenuates neuropathic pain [40]. CCL2-depleted microglia switch from a pro- to anti-inflammatory phenotype and demonstrate reduced migration and invasion properties. CCL2 also can activate spinal microglia when injected intrathecally and trigger behavioral patterns consistent with neuropathic pain [41]. Interestingly, our prior work showed that HuR is a major positive regulator of CCR2, the main receptor for CCL2, in microglia and macrophages [8]. This is consistent with the >60% attenuation of *CCR2* mRNA levels at the epicenter with SRI-42127 treatment. *CCR2* knock-out abrogates neuropathic pain after nerve injury, which may tie into the attenuation of pain observed here [42, 43]. Of note, the fold suppression of *CCR2* mRNA with drug treatment was even greater at rostral and caudal levels (~6-fold) due to the higher expression of *CCR2* mRNA in vehicle controls at those levels. This difference is likely due to injury-related loss of neurons, astrocytes, and oligodendrocytes, all of which express CCR2 [44].

Interestingly, *TGF-β1* was not induced at 8 h post injury or altered with SRI-42127 treatment but increased by ~5-fold in vehicle-treated mice at 5 days. This timeframe is consistent with a prior report where *TGF-β1* induction occurred more gradually (over days) after SCI [45]. In prior studies, we did not see suppression of *TGF-β1* in brain or spinal cord tissues in mice treated with SRI-42127 [10, 16] and so the increase observed here may relate to enhanced glial scar signaling pathways due to a larger lesion size. *TGF-β1* promotes astrocyte proliferation and glial scar formation, and the 5-day timepoint represents the early stage of that process [46–48].

In SCI (and other forms of CNS trauma), there is a rapid peripheral response in organs such as the liver and spleen that strongly influences the proinflammatory microenvironment in the injured cord by promoting mobilization and recruitment of inflammatory monocyte/macrophages and neutrophils [27, 28, 49–52]. In the liver and spleen, there is production and release of chemokines CXCL1 and CCL2 that drive this recruitment. Consistent

with prior reports [50, 52], we observed a significant increase in circulating CXCL1 at the early timepoint of 8 h post injury, with liver tissue showing a ~15-fold induction of *CXCL1* mRNA. SRI-42127 potently suppressed both hepatic mRNA induction and circulating levels of CXCL1. Although early induction of *CCL2* in the liver has been observed with a compression injury model [51, 53], we did not see this at 8 h in our model. On the other hand, circulating CCL2 levels were increased, and spleen tissue showed a selective ~15-fold induction of *CCL2* mRNA. A prior report identified the spleen as the major source for monocyte-derived macrophages recruited to the injured spinal cord, and pre-SCI splenectomy led to improved recovery [54]. The induction of CCL2 after SCI was attributable to myeloid populations within the spleen that can express this chemokine [55], but it may serve as a signal for mobilizing and recruiting bone marrow derived monocytes that eventually infiltrate the injured spinal cord. HuR is expressed by multiple myeloid and non-myeloid cell populations in the periphery [56] and thus would be susceptible to the inhibitory effects of SRI-42127.

IL-6 was induced both in liver and splenic tissues in conjunction with a very large increase in circulating levels. In liver, IL-6 induction is a component of inflammation that has been observed in animal models of acute SCI [49]. Selective induction of IL-6 in liver and spleen (versus TNF-α and IL-1β) has been observed in other models of immune activation [57, 58] although the mechanism remains unclear. Our findings do suggest, however, that these organs are major contributors to circulating IL-6 in early SCI. In humans, elevated serum IL-6 has been detected in the acute phase of SCI, with some studies correlating levels with clinical severity of injury (see review [59]). The attenuation of systemic IL-6 by SRI-42127 may also have contributed to the reduction in pain after SCI as discussed above. Taken together, the suppression of peripheral inflammatory responses by SRI-42127 underscores the broad reach of HuR in cell types outside of the CNS [4, 56].

The effectiveness of SRI-42127 in blocking the inflammatory cascade is borne out by the significantly improved histological and behavioral outcomes. There was attenuation of microglial and astrocyte activation in the injured spinal cord and reduced lesion size with sparing of neurons and white matter. Interestingly, we also observed a significant increase in myelin sparing in rostral and caudal levels in SRI-treated mice. Loss of myelin in these levels is likely related to Wallerian degeneration of white matter tracts both rostral and caudal to injury, reflective of distal axonal degeneration due to separation of axons from their cell bodies [47, 60].

In our prior work, we found that SRI-42127 penetrates the CNS to therapeutic concentrations within 10–15 min after systemic delivery [13] and rapidly suppresses neuroinflammatory responses [10]. These are favorable features for clinical translation in acute SCI where “time is spine” has emerged as a central theme in clinical management [6]. Because SRI-42127 can be administered systemically, it could be given in the field by emergency personnel shortly after injury. In our experimental paradigm, SRI-42127 was given 1 h after SCI for a duration of 5 days.

Neuroinflammatory responses, including activated microglia, astrocytes, and macrophages, persist in chronic phases when

their role switches to a restorative one, promoting neural plasticity, angiogenesis, and stem cell proliferation [3, 61, 62]. HuR regulates trophic factors that promote these restorative functions such as Hif-1 α , VEGF, and GM-CSF, so prolonged treatment with SRI-42127 may be harmful [32, 56, 63–65]. Even IL-6 signaling may promote SCI recovery and neural regeneration [59]. However, the major deleterious proinflammatory mediators that are regulated by HuR approach pre-injury levels by 7 days, providing a time frame for intervention with HuR inhibitors. Further studies will be required to delineate the optimal duration for SRI-42127 treatment after SCI.

Author Contributions

M.A.H., P.H.K., and C.P.C. contributed to the conception and design of the study. M.A.H., R.S., R.E.S., A.K., Y.S., A.Z.H., K.A.S., and J.J.D. performed experiments and acquired data. M.A.H., P.H.K., R.E.S., A.G., S.A.A., L.B.N., and N.F. contributed to data analysis and interpretation. M.A.H. and P.H.K. prepared figures and drafted the manuscript. All authors read and approved the final manuscript.

Acknowledgments

We wish to thank the UAB Animal Behavioral Assessment Core Facility for assistance in testing mice. We also thank Carlos A. Toro, PhD, for helpful discussions regarding methodology.

Conflicts of Interest

The authors declare no conflicts of interest.

Data Availability Statement

The data support the findings of this study and are available on request from the corresponding author. The data are not publicly available due to privacy or ethical restrictions.

References

1. A. Alizadeh, S. M. Dyck, and S. Karimi-Abdolrezaee, “Traumatic Spinal Cord Injury: An Overview of Pathophysiology, Models and Acute Injury Mechanisms,” *Frontiers in Neurology* 10 (2019): 282.
2. J. Bennett, J. M. Das, and P. D. Emmady, “Spinal Cord Injuries,” in *StatPearls (Internet)* (StatPearls Publishing LLC, 2024).
3. D. J. Hellenbrand, C. M. Quinn, Z. J. Piper, C. N. Morehouse, J. A. Fixel, and A. S. Hanna, “Inflammation After Spinal Cord Injury: A Review of the Critical Timeline of Signaling Cues and Cellular Infiltration,” *Journal of Neuroinflammation* 18 (2021): 284.
4. A. Guha, M. A. Husain, Y. Si, et al., “RNA Regulation of Inflammatory Responses in Glia and Its Potential as a Therapeutic Target in Central Nervous System Disorders,” *Glia* 71 (2023): 485–508.
5. H. Kumar, A. E. Ropper, S. H. Lee, and I. Han, “Propitious Therapeutic Modulators to Prevent Blood-Spinal Cord Barrier Disruption in Spinal Cord Injury,” *Molecular Neurobiology* 54 (2017): 3578–3590.
6. C. S. Ahuja, J. R. Wilson, S. Nori, et al., “Traumatic Spinal Cord Injury,” *Nature Reviews. Disease Primers* 3 (2017): 17018.
7. J. Wang, J. W. Leavenworth, A. B. Hjelmeland, et al., “Deletion of the RNA Regulator HuR in Tumor-Associated Microglia and Macrophages Stimulates Anti-Tumor Immunity and Attenuates Glioma Growth,” *Glia* 67 (2019): 2424–2439.
8. P. Matsye, L. Zheng, Y. Si, et al., “HuR Promotes the Molecular Signature and Phenotype of Activated Microglia: Implications for

Amyotrophic Lateral Sclerosis and Other Neurodegenerative Diseases,” *Glia* 65 (2017): 945–963.

9. T. Kwan, C. L. Floyd, S. Kim, and P. H. King, “RNA Binding Protein Human Antigen R Is Translocated in Astrocytes Following Spinal Cord Injury and Promotes the Inflammatory Response,” *Journal of Neurotrauma* 34 (2017): 1249–1259.

10. R. Chellappan, A. Guha, Y. Si, et al., “SRI-42127, a Novel Small Molecule Inhibitor of the RNA Regulator HuR, Potently Attenuates Glial Activation in a Model of Lipopolysaccharide-Induced Neuroinflammation,” *Glia* 70 (2022): 155–172.

11. T. Kwan, C. L. Floyd, J. Patel, A. Mohaimany-Aponte, and P. H. King, “Astrocytic Expression of the RNA Regulator HuR Accentuates Spinal Cord Injury in the Acute Phase,” *Neuroscience Letters* 651 (2017): 140–145.

12. H. Guo, M. Du, Y. Yang, et al., “Sp1 Regulates the M1 Polarization of Microglia Through the HuR/NF-kappaB Axis After Spinal Cord Injury,” *Neuroscience* 544 (2024): 50–63.

13. N. Filippova, X. Yang, S. Ananthan, et al., “Targeting the HuR Oncogenic Role With a New Class of Cytoplasmic Dimerization Inhibitors,” *Cancer Research* 81 (2021): 2220–2233.

14. N. Filippova, X. Yang, S. Ananthan, et al., “Hu Antigen R (HuR) Multimerization Contributes to Glioma Disease Progression,” *Journal of Biological Chemistry* 292 (2017): 16999–17010.

15. N. C. Meisner, M. Hintersteiner, K. Mueller, et al., “Identification and Mechanistic Characterization of Low-Molecular-Weight Inhibitors for HuR,” *Nature Chemical Biology* 3 (2007): 508–515.

16. R. E. Sorge, Y. Si, L. A. Norian, et al., “Inhibition of the RNA Regulator HuR by SRI-42127 Attenuates Neuropathic Pain After Nerve Injury Through Suppression of Neuroinflammatory Responses,” *Neurotherapeutics* 19 (2022): 1649–1661.

17. F. Guida, D. De Gregorio, E. Palazzo, et al., “Behavioral, Biochemical and Electrophysiological Changes in Spared Nerve Injury Model of Neuropathic Pain,” *International Journal of Molecular Sciences* 21, no. 9 (2020): 3396, <https://doi.org/10.3390/ijms21093396>.

18. J. M. Ziebell, P. D. Adelson, and J. Lifshitz, “Microglia: Dismantling and Rebuilding Circuits After Acute Neurological Injury,” *Metabolic Brain Disease* 30 (2015): 393–400.

19. W. J. Streit, S. A. Walter, and N. A. Pennell, “Reactive Microgliosis,” *Progress in Neurobiology* 57 (1999): 563–581.

20. D. M. Basso, L. C. Fisher, A. J. Anderson, L. B. Jakeman, D. M. McTigue, and P. G. Popovich, “Basso Mouse Scale for Locomotion Detects Differences in Recovery After Spinal Cord Injury in Five Common Mouse Strains,” *Journal of Neurotrauma* 23 (2006): 635–659.

21. S. Ito, Y. Kakuta, K. Yoshida, et al., “A Simple Scoring of Beam Walking Performance After Spinal Cord Injury in Mice,” *PLoS One* 17 (2022): e0272233.

22. D. J. Langford, A. L. Bailey, M. L. Chanda, et al., “Coding of Facial Expressions of Pain in the Laboratory Mouse,” *Nature Methods* 7, no. 6 (2010): 447–449, <https://doi.org/10.1038/nmeth.1455>.

23. T. R. F. Green, S. M. Murphy, and R. K. Rowe, “Comparisons of Quantitative Approaches for Assessing Microglial Morphology Reveal Inconsistencies, Ecological Fallacy, and a Need for Standardization,” *Scientific Reports* 12 (2022): 18196.

24. J. Reddaway, P. E. Richardson, R. J. Bevan, J. Stoneman, and M. Palombo, “Microglial Morphometric Analysis: So Many Options, So Little Consistency,” *Frontiers in Neuroinformatics* 17 (2023): 1211188.

25. D. A. Dixon, N. D. Tolley, P. H. King, et al., “Altered Expression of the mRNA Stability Factor HuR Promotes Cyclooxygenase-2 Expression in Colon Cancer Cells,” *Journal of Clinical Investigation* 108 (2001): 1657–1665.

26. S. J. Cok and A. R. Morrison, "The 3'-Untranslated Region of Murine Cyclooxygenase-2 Contains Multiple Regulatory Elements That Alter Message Stability and Translational Efficiency," *Journal of Biological Chemistry* 276 (2001): 23179–23185.
27. D. C. Anthony and Y. Couch, "The Systemic Response to CNS Injury," *Experimental Neurology* 258 (2014): 105–111.
28. B. T. Noble, F. H. Brennan, and P. G. Popovich, "The Spleen as a Neuroimmune Interface After Spinal Cord Injury," *Journal of Neuroimmunology* 321 (2018): 1–11.
29. R. C. Sterner and R. M. Sterner, "Immune Response Following Traumatic Spinal Cord Injury: Pathophysiology and Therapies," *Frontiers in Immunology* 13 (2022): 1084101, <https://doi.org/10.3389/fimmu.2022.1084101>.
30. M. A. Anwar, T. S. Al Shehaby, and A. H. Eid, "Inflammogenesis of Secondary Spinal Cord Injury," *Frontiers in Cellular Neuroscience* 10 (2016): 98, <https://doi.org/10.3389/fncel.2016.00098>.
31. I. Moraga, J. Spangler, J. L. Mendoza, and K. C. Garcia, "Multifarious Determinants of Cytokine Receptor Signaling Specificity," *Advances in Immunology* 121 (2014): 1–39.
32. A. Guha, S. Waris, L. B. Nabors, et al., "The Versatile Role of HuR in Glioblastoma and Its Potential as a Therapeutic Target for a Multi-Pronged Attack," *Advanced Drug Delivery Reviews* 181 (2022): 114082.
33. I. Bonomo, G. Assoni, V. La Pietra, et al., "HuR Modulation With Tanshinone Mimics Impairs LPS Response in Murine Macrophages," *Disease Models & Mechanisms* 16 (2023): dmm.050120.
34. J. Guptarak, S. Wanchoo, J. Durham-Lee, et al., "Inhibition of IL-6 Signaling: A Novel Therapeutic Approach to Treating Spinal Cord Injury Pain," *Pain* 154 (2013): 1115–1128.
35. T. Murakami, T. Kanchiku, H. Suzuki, et al., "Anti-Interleukin-6 Receptor Antibody Reduces Neuropathic Pain Following Spinal Cord Injury in Mice," *Experimental and Therapeutic Medicine* 6 (2013): 1194–1198.
36. J. Y. Lee, C. S. Park, K. J. Seo, et al., "IL-6/JAK2/STAT3 Axis Mediates Neuropathic Pain by Regulating Astrocyte and Microglia Activation After Spinal Cord Injury," *Experimental Neurology* 370 (2023): 114576.
37. H. Ji, Y. Zhang, C. Chen, et al., "D-Dopachrome Tautomerase Activates COX2/PGE(2) Pathway of Astrocytes to Mediate Inflammation Following Spinal Cord Injury," *Journal of Neuroinflammation* 18 (2021): 130.
38. B. Chelluboina, K. R. Nalamolu, J. D. Klopfenstein, et al., "MMP-12, a Promising Therapeutic Target for Neurological Diseases," *Molecular Neurobiology* 55 (2018): 1405–1409.
39. J. Wang, A. B. Hjelmeland, L. B. Nabors, and P. H. King, "Anti-Cancer Effects of the HuR Inhibitor, MS-444, in Malignant Glioma Cells," *Cancer Biology & Therapy* 20 (2019): 979–988.
40. Q. Li, Z. Yang, K. Wang, Z. Chen, and H. Shen, "Suppression of Microglial Ccl2 Reduces Neuropathic Pain Associated With Chronic Spinal Compression," *Frontiers in Immunology* 14 (2023): 1191188.
41. M. A. Thacker, A. K. Clark, T. Bishop, et al., "CCL2 Is a Key Mediator of Microglia Activation in Neuropathic Pain States," *European Journal of Pain* 13, no. 3 (2009): 263–272, <https://doi.org/10.1016/j.ejpain.2008.04.017>.
42. M. Ma, T. Wei, L. Boring, I. F. Charo, R. M. Ransohoff, and L. B. Jakeman, "Monocyte Recruitment and Myelin Removal Are Delayed Following Spinal Cord Injury in Mice With CCR2 Chemokine Receptor Deletion," *Journal of Neuroscience Research* 68 (2002): 691–702.
43. C. Abbadie, J. A. Lindia, A. M. Cumiskey, et al., "Impaired Neuropathic Pain Responses in Mice Lacking the Chemokine Receptor CCR2," *Proceedings of the National Academy of Sciences of the United States of America* 100 (2003): 7947–7952.
44. G. Banisadr, F. Queraud-Lesaux, M. C. Bouterin, et al., "Distribution, Cellular Localization and Functional Role of CCR2 Chemokine Receptors in Adult Rat Brain," *Journal of Neurochemistry* 81, no. 2 (2002): 257–269, <https://doi.org/10.1046/j.1471-4159.2002.00809.x>.
45. M. Joko, K. Osuka, N. Usuda, K. Atsuzawa, M. Aoyama, and M. Takayasu, "Different Modifications of Phosphorylated Smad3C and Smad3L Through TGF-Beta After Spinal Cord Injury in Mice," *Neuroscience Letters* 549 (2013): 168–172.
46. L. Gong, Y. Gu, X. Han, et al., "Spatiotemporal Dynamics of the Molecular Expression Pattern and Intercellular Interactions in the Glial Scar Response to Spinal Cord Injury," *Neuroscience Bulletin* 39 (2023): 213–244.
47. A. Shafqat, I. Albalkhi, H. M. Magableh, T. Saleh, K. Alkattan, and A. Yaqinuddin, "Tackling the Glial Scar in Spinal Cord Regeneration: New Discoveries and Future Directions," *Frontiers in Cellular Neuroscience* 17 (2023): 1180825.
48. C. W. Ma, Z. Q. Wang, R. Ran, et al., "TGF-Beta Signaling Pathway in Spinal Cord Injury: Mechanisms and Therapeutic Potential," *Journal of Neuroscience Research* 102 (2024): e25255.
49. M. T. Goodus and D. M. McTigue, "Hepatic Dysfunction After Spinal Cord Injury: A Vicious Cycle of Central and Peripheral Pathology?," *Experimental Neurology* 325 (2020): 113160.
50. A. G. Yates, T. Jogia, E. R. Gillespie, Y. Couch, M. J. Ruitenberg, and D. C. Anthony, "Acute IL-1RA Treatment Suppresses the Peripheral and Central Inflammatory Response to Spinal Cord Injury," *Journal of Neuroinflammation* 18 (2021): 15.
51. S. J. Campbell, V. H. Perry, F. J. Pitossi, et al., "Central Nervous System Injury Triggers Hepatic CC and CXC Chemokine Expression That Is Associated With Leukocyte Mobilization and Recruitment to Both the Central Nervous System and the Liver," *American Journal of Pathology* 166 (2005): 1487–1497.
52. S. J. Campbell, P. M. Hughes, J. P. Iredale, et al., "CINC-1 Is an Acute-Phase Protein Induced by Focal Brain Injury Causing Leukocyte Mobilization and Liver Injury," *FASEB Journal* 17 (2003): 1168–1170.
53. C. D'Mello, T. Le, and M. G. Swain, "Cerebral Microglia Recruit Monocytes Into the Brain in Response to Tumor Necrosis Factoralpha Signaling During Peripheral Organ Inflammation," *Journal of Neuroscience* 29 (2009): 2089–2102.
54. L. V. Blomster, F. H. Brennan, H. W. Lao, D. W. Harle, A. R. Harvey, and M. J. Ruitenberg, "Mobilisation of the Splenic Monocyte Reservoir and Peripheral CX3CR1 Deficiency Adversely Affects Recovery From Spinal Cord Injury," *Experimental Neurology* 247 (2013): 226–240, <https://doi.org/10.1016/j.expneurol.2013.05.002>.
55. M. Gschwandtner, R. Derler, and K. S. Midwood, "More Than Just Attractive: How CCL2 Influences Myeloid Cell Behavior Beyond Chemotaxis," *Frontiers in Immunology* 10 (2019): 2759.
56. S. Srikantan and M. Gorospe, "HuR Function in Disease," *Frontiers in Bioscience-Landmark* 17, no. 1 (2012): 189–205, <https://doi.org/10.2741/3921>.
57. P. Szot, A. Franklin, D. P. Figlewicz, et al., "Multiple Lipopolysaccharide (LPS) Injections Alter Interleukin 6 (IL-6), IL-7, IL-10 and IL-6 and IL-7 Receptor mRNA in CNS and Spleen," *Neuroscience* 355 (2017): 9–21.
58. X. L. Zhu, N. D. Pacheco, E. J. Dick, and F. M. Rollwagen, "Differentially Increased IL-6 mRNA Expression in Liver and Spleen Following Injection of Liposome-Encapsulated Haemoglobin," *Cytokine* 11 (1999): 696–703.
59. H. Shipman, M. Monsour, M. M. Foley, S. Marbacher, D. M. Croci, and E. F. Bisson, "Interleukin-6 in Spinal Cord Injury: Could Immunomodulation Replace Immunosuppression in the Management of Acute Traumatic Spinal Cord Injuries?," *Journal of Neurological Surgery Part A: Central European Neurosurgery* 85 (2024): 602–609.

60. J. Cohen-Adad, H. Leblond, H. Delivet-Mongrain, M. Martinez, H. Benali, and S. Rossignol, "Wallerian Degeneration After Spinal Cord Lesions in Cats Detected With Diffusion Tensor Imaging," *NeuroImage* 57 (2011): 1068–1076.
61. Y. Wu, Z. Tang, J. Zhang, Y. Wang, and S. Liu, "Restoration of Spinal Cord Injury: From Endogenous Repairing Process to Cellular Therapy," *Frontiers in Cellular Neuroscience* 16 (2022): 1077441, <https://doi.org/10.3389/fncel.2022.1077441>.
62. X. Freyermuth-Trujillo, J. J. Segura-Urbe, H. Salgado-Ceballos, C. E. Orozco-Barrios, and A. Coyoy-Salgado, "Inflammation: A Target for Treatment in Spinal Cord Injury," *Cells* 11 (2022): 2692.
63. Y. Li, W. Han, Y. Wu, et al., "Stabilization of Hypoxia Inducible Factor-1alpha by Dimethyloxalylglycine Promotes Recovery From Acute Spinal Cord Injury by Inhibiting Neural Apoptosis and Enhancing Axon Regeneration," *Journal of Neurotrauma* 36 (2019): 3394–3409.
64. C. Zamanian, G. Kim, C. Onyedimma, et al., "A Review of Vascular Endothelial Growth Factor and Its Potential to Improve Functional Outcomes Following Spinal Cord Injury," *Spinal Cord* 61 (2023): 231–237.
65. J. W. Tao, X. Fan, J. Y. Zhou, et al., "Granulocyte Colony-Stimulating Factor Effects on Neurological and Motor Function in Animals With Spinal Cord Injury: A Systematic Review and Meta-Analysis," *Frontiers in Neuroscience* 17 (2023): 1168764.

Supporting Information

Additional supporting information can be found online in the Supporting Information section.